

Quantum fisher information protection of N -qubit Greenberger-Horne-Zeilinger state from decoherence

Sajede Harraz¹, Shuang Cong¹, Jiaoyang Zhang¹ and Juan J. Nieto²

¹ Department of Automation, University of Science and Technology of China, Hefei 230027, China

² Instituto de Matematicas, CITMaga, Universidade de Santiago de Compostela, 15782 Santiago de Compostela, Spain

E-mail: sajede@ustc.edu.cn

Abstract. In this paper we study the protection of N -qubit Greenberger-Horne-Zeilinger (GHZ) state and generalized N -qubit GHZ states in amplitude damping channel by means of quantum weak measurement and flip operations. We derive the explicit formulas of the performances of the protection scheme: average fidelity, average probability and the average quantum fisher information (QFI). Moreover, the analytical results for maximizing the average fidelity and probability are obtained. We show that our scheme can effectively protect the average QFI of phase for GHZ states and generalized GHZ states. The proposed scheme has the merit of protecting GHZ state and the QFI of phase against heavy amplitude damping noise. Further we show that for some generalize GHZ state, the proposed scheme can protect the state with probability one and fidelity more than 99%.

Keywords: Quantum fisher information, quantum state protection, decoherence, weak measurement.

1. Introduction

One of the basic tasks in information theory is parameter estimation of probability distributions, which has been generalized to quantum systems [1, 2]. The Fisher information as a central role in estimation theory measures the amount of information of a parameter that we can extract from a probability distribution. By larger fisher information one can estimate the parameter more accurately. Since the characteristic of quantum mechanics is probabilistic, fisher information can be extended to quantum regime. Quantum fisher information (QFI) is defined in Cramer-Rao bound $\delta\phi \geq 1/\sqrt{vF}$, where ϕ is the parameter to be estimated, v the measurement times and F is the QFI [3]. Hence, obtaining large QFI is a crucial task in quantum control.

However, the inevitable interaction with environment in real quantum systems, which cause decoherence, needs to be taken into account [4]. One of the important noise sources is amplitude damping which occurs in many quantum systems [5], such as a photon qubit in a leaky cavity, an atomic qubit subjected to spontaneous decay, or a super-conduction qubit with zero-temperature energy relaxation. Various strategies are studied to overcome the effects of decoherence, such as: quantum error correction [6, 7, 8, 9, 10, 11], decoherence-free subspaces [12, 13], quantum feedback control (QFBC) [14, 15, 16, 17, 18, 19] and quantum feed-forward control (QFFC) [20, 21, 22]. To protect the state from environmental noise, a quantum feedback control was proposed by using weak measurements and rotation operation after the noise channel in [15]. This scheme is experimentally implemented in [16] and is considered for protection of arbitrary initial states against different types of noise sources [23, 24]. Quantum feedback control applies control operations after the noise channel, while quantum feed-forward control is about control operations both before and after noise channel. The aim to apply operations before noise is to make the state immune to the effects of the noise channel. Hence, one needs to know the characteristics of the noise. In [20] a quantum feed-forward control is proposed to protect the state from amplitude damping, and was extended to protect two-qubit systems from amplitude damping channel (ADC) [25]. This scheme is also considered for discrimination of two non-orthogonal states against noise [22].

In quantum systems, any measurement comes with a price which is disturbance of the system [26, 27]. However, by quantum weak measurement one can find a trade-off between information gain and disturbing it through measurement. The basic idea of the weak measurement is that the interaction (or disturbance) between the measuring apparatus and the observed system or particle is so weak, that the wave function does not collapse but continues unchanged [28]. In both QFBC and QFFC schemes, the weak measurement with an optimum measurement strength is used to find the optimal protection from noise.

In this paper we study the protection of the average QFI and the state of N -qubit Greenberger–Horne–Zeilinger (GHZ) state from ADC by means of weak measurement and offsetting operations. The control procedure consists of pre and post noise channel operations. Hence, we call the proposed scheme as quantum feed-forward control and its reversal (QFFCR) hereafter. Before noise channel, a weak measurement applies to gain information about the state of the system. Then according to the result of the measurement, we apply an offsetting operation to make the state less vulnerable to the effect of ADC. After the noise channel, the aim is to retrieve the state, so the same offsetting operation as the one before the noise channel is applied. Finally, to bring the state as close as possible to its initial state we apply a correction rotation at the final step of the protection control. Although the final states of the scheme for N -qubit is different (there are 2^N kind results of the final state which come from the 2^N kind measurement results of the weak measurement), they have the same structure, so we can calculate the average QFI, average fidelity and average success probability analytically. We derive the final expressions for three performances of the control: average total QFI,

fidelity and probability of N -qubit generalized GHZ states; and study the optimum parameters to gain maximum of each performances of the proposed control scheme. Our scheme can protect not only GHZ states but also some generalized GHZ states. The simulation results show that by using optimum parameters, the proposed QFFCR scheme can protect some generalized GHZ states with probability 1 and fidelity close to 1 even for intense decaying rates.

For comparison, we discuss another scheme that uses weak-measurement-based pre- and post-flips (WMPPF) [30] and demonstrate by the simulation results that our scheme has much better performance. In WMPPF scheme the state is measured by WM operators before the noise channel, and the flips are applied according to the result of the WM to make the state almost immune to the effects of the noise. Then, after the noise channel the reversed flips are applied to recover the state. The WMPPF has the success probability equal to 1 for all decaying rates and measurement strengths while the QFFCR is a probabilistic scheme.

This paper is organized as follows: In Sec. 2, we define the QFFCR scheme for one-qubit protection. Sec. 3 is the protection scheme performance derivations of N -qubit generalized GHZ state, including average total probability, fidelity and QFI. In Sec. 4, we do the numerical simulations and study the behavior of QFFCR performances for protection of N -qubit GHZ state in ADC. Finally, in Sec. 5 we give the conclusion of our results.

2. Noise protection control scheme for one-qubit

The protection scheme is divided into two parts, the operations before the noise channel, which are the weak measurement and offsetting operations; and the operations after the noise channel, which are the offsetting and rotation operations, respectively. The aim of before noise operations is to make the state almost immune to the effect of noise channel and by after noise operations, we try to retrieve the state and bring it back as close as possible to its initial state.

The whole process of state protection consists of 5 steps, which is shown in Fig. 1 and is explained in the following [29].

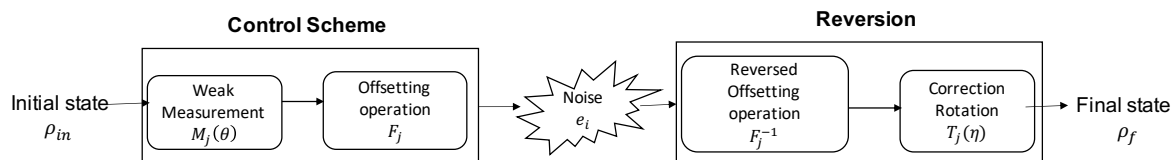


Figure 1. Schematic diagram of QFFCR.

Step 1: In the first step, we apply the weak measurement as $\Pi_0 = M_0^\dagger M_0$ and $\Pi_1 = M_1^\dagger M_1$ to gain some information about the system. The weak measurement

operators are along z -axis of the Bloch sphere as:

$$\begin{aligned} M_0 &= \cos(\theta/2)|0\rangle\langle 0| + \sin(\theta/2)|1\rangle\langle 1| \\ M_1 &= \sin(\theta/2)|0\rangle\langle 0| + \cos(\theta/2)|1\rangle\langle 1| \end{aligned} \quad (1)$$

where $\theta \in [0, \frac{\pi}{2}]$ and the strength of the measurement is defined by the angle θ . When $\theta = \pi/2$, the strength of the measurement is zero, and we call it as: “no measurement” (NM) scheme. When $\theta = 0$, the strength of the measurement is maximum and is called as “projective measurement” (PM), in a way that the state of the system projected onto the state $|0\rangle$ (or $|1\rangle$) when the measurement result is 0 (or 1). When $0 < \theta < \pi/2$, we call it as “weak measurement” (WM) scheme. Hence, we can adjust the strength of the measurement for the trade-off between the information gain and disturbance of the system because of measurement.

Step 2: According to the result of the measurement, the offsetting operations are applied to make the state immune to the effect of noise before ADC.

$$F_0 = I = \begin{pmatrix} 1 & 0 \\ 0 & 1 \end{pmatrix}, \quad F_1 = \sigma_x = \begin{pmatrix} 0 & 1 \\ 1 & 0 \end{pmatrix} \quad (2)$$

where $F_0 (F_1)$ corresponds to the result of the measurement operator $M_0 (M_1)$ respectively. When the result corresponds to measurement operator M_0 is acquired, the state is close to the ground state, so noise will not have much effects on the state. Therefore, in offsetting step we do not need to make changes in the state, and F_0 is chosen as identity operator. However, when the result corresponds to measurement operator M_1 is acquired, by applying the operator F_1 , the state of the system becomes closer to the ground state and less vulnerable to the effects of noise.

Step 3: In this step, the state of the system is ready to enter the ADC. For each qubit the amplitude damping is represented by Kraus operators as:

$$e_0 = \begin{pmatrix} 1 & 0 \\ 0 & \sqrt{1-r} \end{pmatrix}, \quad e_1 = \begin{pmatrix} 0 & \sqrt{r} \\ 0 & 0 \end{pmatrix} \quad (3)$$

where $r \in [0, 1]$ is the possibility of decaying of the excited state with $r = e^{-\Gamma t}$, Γ is the energy relaxation rate and t is the evolving time [31].

Step 4: After the ADC, the same offsetting operations as given in Eq. (2) are applied.

Step 5: At the final step, to correct the state and bring it back to its initial state, the correction rotation is applied as:

$$T_0 = \begin{pmatrix} e^{i\frac{\eta}{2}} & 0 \\ 0 & e^{-i\frac{\eta}{2}} \end{pmatrix}, \quad T_1 = \begin{pmatrix} e^{-i\frac{\eta}{2}} & 0 \\ 0 & e^{i\frac{\eta}{2}} \end{pmatrix} \quad (4)$$

where $T_0 (T_1)$ corresponds to the result of measurement operator $M_0 (M_1)$, respectively.

3. Protection scheme Performance Derivations of N -qubit generalized GHZ state

Here we give the average QFI, average fidelity and average probability of proposed QFFCR for general N -qubit GHZ state. The initial state in this paper is the N -qubit generalized GHZ state as

$$|\psi_{in}\rangle = \alpha|0\rangle^{\otimes N} + \beta|1\rangle^{\otimes N} \quad (5)$$

where $\alpha = \cos(\gamma/2)$, $\beta = e^{i\phi_0} \sin(\gamma/2)$, $0 < \gamma < 1$, and ϕ_0 is the initial phase. By setting $\gamma = \pi/2$, $\phi_0 = 0$ we gain the GHZ state. Once more, we assume that all the qubits have the same control parameters, same weak measurement strength, same damping probability and same rotation angle.

The normalized final state of QFFCR is attainable, in which there are 2^N different final states according to 2^N different kind of measurement results. Fortunately, all different results of final states have the same structure as

$$\rho_f = \frac{1}{P} \tilde{\rho} = \frac{1}{P} \begin{pmatrix} A & 0 & D \\ 0 & E & 0 \\ C & 0 & B \end{pmatrix} \quad (6)$$

where $\tilde{\rho}$ is the unnormalized final state and P is the average total probability of appearing ρ_f .

The detailed calculation of the elements of A , B , C , D and E matrix of N -qubit GHZ state in Eq. (6) at each step in QFFCR is given in **Appendix**. Here we calculate the average total probability, fidelity and QFI.

3.1. Average total probability

For the normalized final state Eq. (6) the total probability is calculated as

$$P = \text{Tr}(\tilde{\rho}) = A + B + \text{Tr}(E) \quad (7)$$

Hence, the average total probability is the sum of the probabilities of three cases, $k = 0$, $k = N$ and $k = 1$ to $N - 1$.

$$\begin{aligned} P_0 &= A_0 + B_0 + \text{Tr}(E_0) = \\ &\alpha^2 \sin^{2N} \left(\frac{\theta}{2} \right) (re^{Ni\eta} + (1-r)e^{-Ni\eta})^N + \beta^2 \cos^{2N} \left(\frac{\theta}{2} \right) e^{Ni\eta} \\ P_N &= A_N + B_N + \text{Tr}(E_N) = \\ &\alpha^2 \cos^{2N} \left(\frac{\theta}{2} \right) e^{Ni\eta} + \beta^2 \sin^{2N} \left(\frac{\theta}{2} \right) (re^{i\eta} + (1-r)e^{-i\eta})^N \\ P_{S_k} &= A_{S_k} + B_{S_k} + \text{Tr}(E_{S_k}) = \\ &\alpha^2 \sin^{2(N-k)} \left(\frac{\theta}{2} \right) \cos^{2k} \left(\frac{\theta}{2} \right) e^{ki\eta} (re^{i\eta} + (1-r)e^{-i\eta})^{N-k} + \\ &\beta^2 \cos^{2(N-k)} \left(\frac{\theta}{2} \right) e^{(N-k)i\eta} \sin^{2k} \left(\frac{\theta}{2} \right) (re^{i\eta} + (1-r)e^{-i\eta})^{N-k} \end{aligned} \quad (8)$$

When $k = 1$ to $N - 1$, there are C_N^k kind cases, so the average total probability becomes

$$\begin{aligned}
 P_{total} &= P_0 + P_N + \sum_{k=1}^{N-1} \sum_{lk=1}^{C_N^k} P_{lk} = (re^{i\eta} + (1-r)e^{-i\eta})^N \sin^{2N} \left(\frac{\theta}{2} \right) + \\
 &\cos^{2N} \left(\frac{\theta}{2} \right) e^{iN\eta} + \sum_{k=1}^{N-1} \frac{N!}{k!(N-k)!} P_{lk} = \\
 &\left((re^{i\eta} + (1-r)e^{-i\eta}) \sin^2 \left(\frac{\theta}{2} \right) + e^{i\eta} \cos^2 \left(\frac{\theta}{2} \right) \right)^N
 \end{aligned} \tag{9}$$

3.2. Average total fidelity

The fidelity between initial state $|\psi_{in}\rangle$ Eq. (5) and final state ρ_f Eq. (6) is given as

$$Fid = \langle \psi_{in} | \rho_f | \psi_{in} \rangle = \frac{1}{P} (|\alpha|^2 A + \alpha\beta^* C + \alpha^* \beta D + |\beta|^2 B) \tag{10}$$

where P is the average total probability. The fidelities in three cases of $k = 0$, $k = N$ and $k = 1$ to $N - 1$ are

$$\begin{aligned}
 Fid_0 &= \frac{1}{p_0} (|\alpha|^2 A_0 + \alpha\beta^* C_0 + \alpha^* \beta D_0 + |\beta|^2 B_0); \\
 Fid_N &= \frac{1}{p_0} (|\alpha|^2 A_N + \alpha\beta^* C_N + \alpha^* \beta D_N + |\beta|^2 B_N); \\
 Fid_{S_k} &= \frac{1}{p_0} (|\alpha|^2 A_{S_k} + \alpha\beta^* C_{S_k} + \alpha^* \beta D_{S_k} + |\beta|^2 B_{S_k});
 \end{aligned} \tag{11}$$

Therefore, the average total fidelity is the sum of the fidelities of three cases, $k = 0$, $k = N$ and $k = 1$ to $N - 1$ as:

$$\begin{aligned}
 Fid_{total} &= \frac{1}{p_{total}} \left[P_0 Fid_0 + P_N Fid_N + \sum_{k=1}^{N-1} \sum_{S_k=1}^{C_N^k} P_{S_k} Fid_{S_k} \right] \\
 &= \frac{1}{p_{total}} \left[(|\alpha|^2 A_0 + \alpha\beta^* C_0 + \alpha^* \beta D_0 + |\beta|^2 B_0) + \right. \\
 &\quad \left. (|\alpha|^2 A_N + \alpha\beta^* C_N + \alpha^* \beta D_N + |\beta|^2 B_N) + \right. \\
 &\quad \left. \sum_{k=1}^{N-1} \sum_{S_k=1}^{C_N^k} (|\alpha|^2 A_{S_k} + \alpha\beta^* C_{S_k} + \alpha^* \beta D_{S_k} + |\beta|^2 B_{S_k}) \right] \\
 &= \frac{1}{p_{total}} \left[(|\alpha|^4 + |\beta|^4) \left[\cos^2 \left(\frac{\theta}{2} \right) e^{i\eta} + \sin^2 \left(\frac{\theta}{2} \right) e^{-i\eta} (1-r) \right]^N + \right. \\
 &\quad \left. 2|\alpha\beta|^2 r^N e^{iN\eta} \sin^{2N} \left(\frac{\theta}{2} \right) + 2^{N+1} |\alpha\beta|^2 (1-r)^{N/2} \frac{\sin^N(\theta)}{2^N} \right]
 \end{aligned} \tag{12}$$

As the final expression of average total fidelity Eq. (12) shows, there is a trade-off between average total fidelity and probability, so by increasing one, the other will decrease. Hence, one needs to find the best balance between fidelity and probability.

3.3. Average total QFI

In classical definition, fisher information is measuring the amount of information that an observable random variable carries about an unknown parameter σ . The quantum

fisher information is formally generalized from classical fisher information definition as [32, 33]:

$$F_\sigma = \sum_{l'} \frac{(\partial_\sigma \lambda_{l'})^2}{\lambda_{l'}} + \sum_{l \neq m} \frac{2(\lambda_l - \lambda_m)^2}{\lambda_l + \lambda_m} |\langle \varphi_l | \partial_\sigma | \varphi_m \rangle|^2 \quad (13)$$

where $\partial_\sigma \equiv \frac{\partial}{\partial \sigma}$ and $|\varphi_m\rangle$, $|\varphi_l\rangle$ are the eigenvectors and λ the eigenvalues of the state. The first summation is equal to the classical fisher information which is called the classical term and the second summation is called the quantum term.

In this paper, we consider the parameter ϕ_0 phase of the initial state in Eq. (5), as the unknown parameter to be measured and estimated.

As it has been proved in [30], to calculate the QFI of phase ϕ_0 for density matrix with the structure of Eq. (6), Eq. (13) can be simplified as:

$$QFI = \frac{1}{P} \frac{4|C|^2}{A+B} N^2 \quad (14)$$

where A , B and C are the density matrix elements as given in Eq. (6) and N the number of qubits.

Hence the QFI in three cases of $k = 0$, $k = N$ and $k = 1$ to $N - 1$ are

$$QFI_0 = \frac{1}{P_0} \frac{4|C_0|^2}{A_0 + B_0} N^2, \quad QFI_N = \frac{1}{P_N} \frac{4|C_N|^2}{A_N + B_N} N^2, \quad QFI_{S_k} = \frac{1}{P_{S_k}} \frac{4|C_{S_k}|^2}{A_{S_k} + B_{S_k}} N^2 \quad (15)$$

Therefore, the average total QFI of phase of our QFFCR scheme is

$$\begin{aligned} QFI_{total} &= P_0 QFI_0 + P_N QFI_N + \sum_{k=1}^{N-1} \sum_{S_k=1}^{C_N^k} P_{S_k} QFI_{S_k} \\ &= \frac{4|\alpha\beta|^2 (1-r)^N \frac{\sin^{2N}(\frac{\theta}{2})}{2^{2N}} N^2}{|\alpha|^2 \sin^{2N}(\frac{\theta}{2}) (r(1-r))^N + |\beta|^2 \cos^{2N}(\frac{\theta}{2}) e^{N i \eta}} \\ &\quad + \frac{4|\alpha\beta|^2 (1-r)^N \frac{\sin^{2N}(\frac{\theta}{2})}{2^{2N}} N^2}{|\alpha|^2 \cos^{2N}(\frac{\theta}{2}) e^{N i \eta} + |\beta|^2 \sin^{2N}(\frac{\theta}{2}) (r(1-r))^N} + \sum_{k=1}^{N-1} \frac{N!}{k!(N-k)!} \\ &\quad \left(\frac{4|\alpha\beta|^2 (1-r)^N \frac{\sin^{2N}(\frac{\theta}{2})}{2^{2N}} N^2}{|\alpha|^2 \cos^{2k}(\frac{\theta}{2}) \sin^{2(N-k)}(\frac{\theta}{2}) (1-r)^{N-k} e^{(-N+2k)i\eta} + |\beta|^2 \sin^{2k}(\frac{\theta}{2}) (1-r)^k e^{(N-2k)i\eta} \cos^{2(N-k)}(\frac{\theta}{2})} \right) \end{aligned} \quad (16)$$

where $\theta \in [0, \frac{\pi}{2}]$ is the measurement strength, $r \in [0, 1]$ is the decay rate, N is the number of qubits and $k = 0$ to N .

4. QFFCR performances for protection of N -qubit GHZ state in ADC

In this section, the experimental simulation results and analysis of proposed QFFCR protection scheme for N -qubit GHZ state against amplitude damping are given.

As we mentioned before, according to Eq. (12) there is a trade-off between average total probability and average total fidelity. By maximizing one, we get the lowest amount of the other. Hence, we study maximizing each one separately.

According to Eq. (9), Eq. (12) and Eq. (16), the amount $|\beta|$ is appeared in the final derived equations of performances; Hence any value for ϕ_0 will get the same result

for the total average probability, fidelity and QFI. Therefore, we do not consider the value of ϕ_0 in numerical simulations.

First, we do the simulation experiments to find the behavior of average total QFI. The initial state is given in Eq. (5), which is GHZ state when $\gamma = \pi/2$ and is generalized GHZ state (GGHZ) state when $\gamma \neq \pi/2$. To show the effectiveness of our scheme, we give the performance comparison with WMPPF scheme proposed in [30].

4.1. Maximum performances

4.1.1. Maximum QFI In this subsection, we study the protection of QFI of phase ϕ_0 of GHZ state by fixing $\gamma = \pi/2$ in Eq. (5). In Fig. 2, the number of qubits is fixed as $N = 10$, the amount of damping probability r is changing from 0 to 1 and the average total QFI is calculated according to Eq. (16). For each amount of damping probability, we find the optimum measurement angle θ and rotation angle η to gain the maximum QFI. When we use the optimum parameters to gain the maximum performance, we call the scheme as maximum QFFCR (MQFFCR). The do nothing (DN) scheme is the case where the states pass through the noise channel without any protection. The corresponding Fidelity and probability of maximum QFI are also given in Fig. 2(c). Also, for comparison, the maximum QFI of WMPPF is given as MWMPF with the same parameters, where the pre weak measurement in WMPPF scheme is optimized to get the optimized QFI.

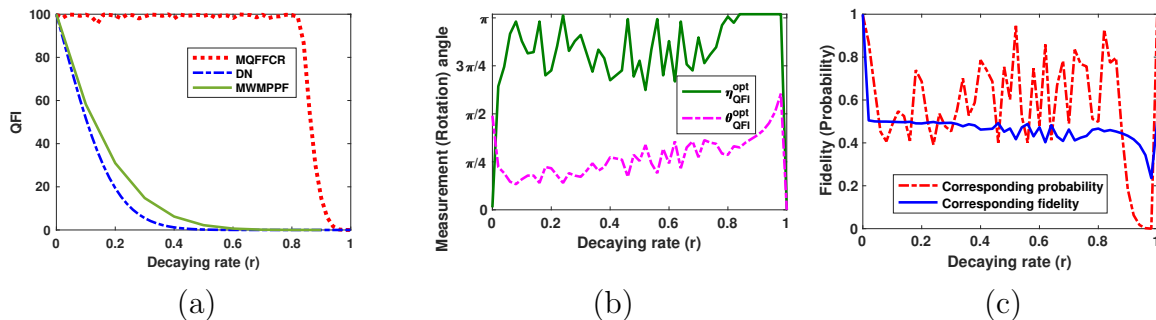


Figure 2. (a) Average total QFI as a function of damping probability. (b) Optimum measurement and rotation angle to gain maximum QFI. (c) Corresponding fidelity and probability.

As Fig. 2(a) depicted, the MQFFCR scheme protects QFI of phase completely and has great improvement over DN case even for intense decaying rates. After decaying rate $r = 0.82$ the amount of QFI decreases and becomes less than 15 for $r = 0.9$. It is easy to find from the Fig. 2(a) that the MQFFCR scheme is all higher than the MWMPF scheme, which means by using the MQFFCR we can highly improve the measurement accuracy of the phase.

Fig. 2(b) is the optimum amounts of measurement angle θ and rotation angle η to obtain maximum QFI. The amount of measurement angle is $0 < \theta < \pi/2$ for most amounts of decaying rate, which means to gain maximum QFI the WM scheme

of measurement operators are applied. In addition, the corresponding fidelity and probability of maximum QFI scheme is given in Fig. 2(c). As one can see from Fig. 2(c), the fidelity of maximum QFI is 0.5 for most decaying rates and the amount of probability is changing between 0.5 to 0.95 for decaying rates $r \leq 0.9$. Hence, protection of QFI, decrease the protection of the state to 50%, and one cannot protect both QFI and fidelity completely at the same time.

4.1.2. Maximum Fidelity Here we study the behavior of maximum fidelity as a function of decaying rate r . The situation is same as Fig. 2, and the average total fidelity is calculated by Eq. (12). Again, for each amount of decaying rate the optimum measurement and rotation angle is used to gain maximum fidelity; hence, we call the scheme as MQFFCR. Fig. 3 shows the maximum fidelity and corresponding probability over 0 to 1 decaying rate. The corresponding measurement and rotation angles are also given.

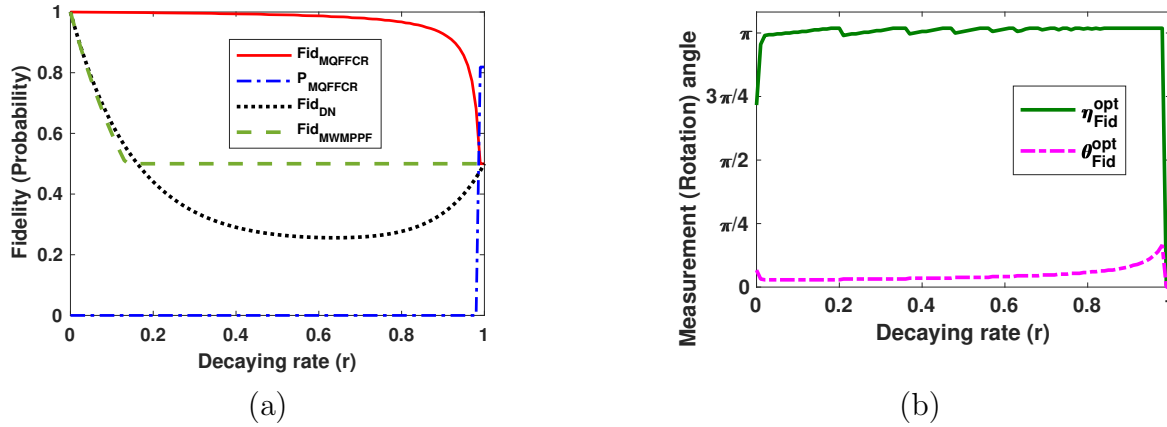


Figure 3. (a) Average total fidelity as a function of damping probability. (b) Optimum measurement and rotation angle to gain maximum QFI.

As Fig. 3 shows, the maximized fidelity of MQFFCR is more than 98% for decaying rates $r \leq 0.7$. For higher decaying rates, the maximized fidelity decreases until it become 0.5 at $r = 1$. As we said before, there is a trade-off between fidelity and probability as shown in Eq. (12), which means by increasing one, the other will decrease. That is why the corresponding probability of maximum fidelity is zero for most decaying rates. In addition, Fig. 3(a) shows that MQFFCR can give much better protection compared to MWMPFF scheme for all decaying rates. Fig. 3 (b) is the optimum rotation and measurement angle to gain maximum fidelity. As Fig. 3 (b) depicted, to gain maximum fidelity the measurement angle must be small which means strong measurement or nearly projective measurement is needed. Also, the amount of rotation angle is near π for most decaying rates.

4.1.3. Maximum probability In this subsection, we give the optimum condition to gain maximum probability. The behavior of maximum probability and corresponding fidelity as a function of decaying rate r is given. The situation is same as Fig. 2, the average total probability is calculated as Eq. (9) and the average total fidelity as Eq. (12). Again, for each damping probability the optimum measurement and rotation angle is used to gain maximum probability; hence, we call the scheme as MQFFCR.

In order to gain maximum probability $P = 1$, the trace of the final density matrix must be $Tr(\rho_f) = 1$. Hence, we derive the optimum rotation angle to gain maximum probability as:

$$\eta_P^{opt}(r, \theta) = -i \log \left(\frac{1 + \sqrt{1 - 4(\cos^2(\theta/2) + r \sin^2(\theta/2))((1-r) * \sin^2(\theta/2))}}{2(\cos^2(\theta/2) + r \sin^2(\theta/2))} \right) \quad (17)$$

We note that, by setting rotation angle as Eq. (17), the amount of probability P is always 1, for all amounts of decaying rate r and measurement angle θ . Therefore, for each r and fixed optimum rotation angle η , we find the maximum fidelity by changing θ from 0 to π and plot the maximum probability and corresponding maximum fidelity as a function of decaying rate r in Fig. 4.

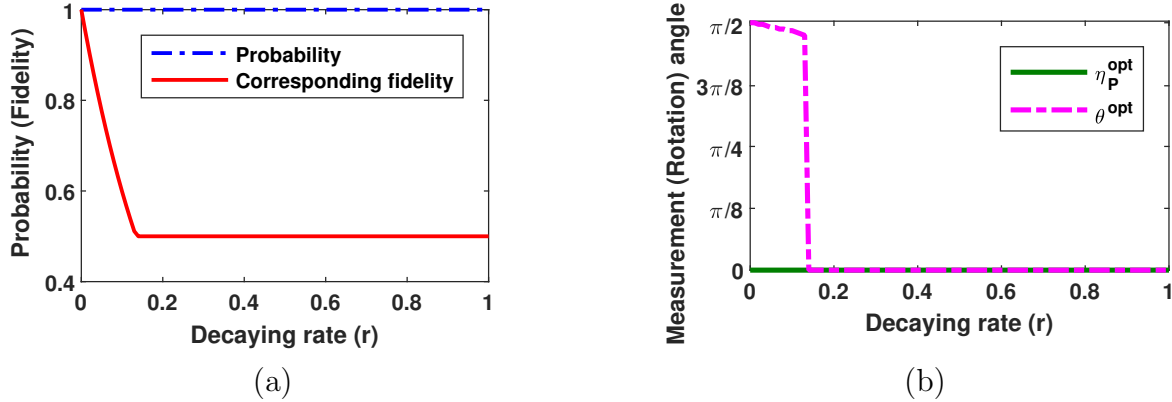


Figure 4. (a) Maximized probability as a function of decaying rate. (b) Optimum measurement and rotation angle to gain maximum probability.

As Fig. 4(a) shows, probability 1 is achievable for all decaying rates. Although, the corresponding fidelity of maximum probability is 0.5 and only for low decaying rates $r \leq 0.15$, we can gain fidelity more than 0.5. As Fig. 4(b) demonstrates, to gain maximum probability for all decaying rates, rotation angle is always equal to 0. In other words, no rotation must apply if one wants to achieve the probability 1. Moreover, the optimum measurement angle for small decaying rates $r \leq 0.15$ is near $\pi/2$, which makes the measurement becomes weak measurement. While for $r > 0.15$ the optimum measurement angle is 0, which makes the measurement becomes projective measurement.

4.1.4. Fidelity and probability comparison As we explained before there is a trade-off between probability and fidelity of our scheme. In this subsection to show the relation between fidelity and probability, we change the amount of measurement and rotation angle from 0 to π and plot corresponding average total fidelity Eq.(12) and average total probability Eq. (9) in Fig. 5 for fixed amounts of decaying rate $r = 0.5$, and 0.9. The blue dots demonstrate the performance of the proposed QFFCR scheme for all independent amounts of measurement angle θ and rotation angle η .

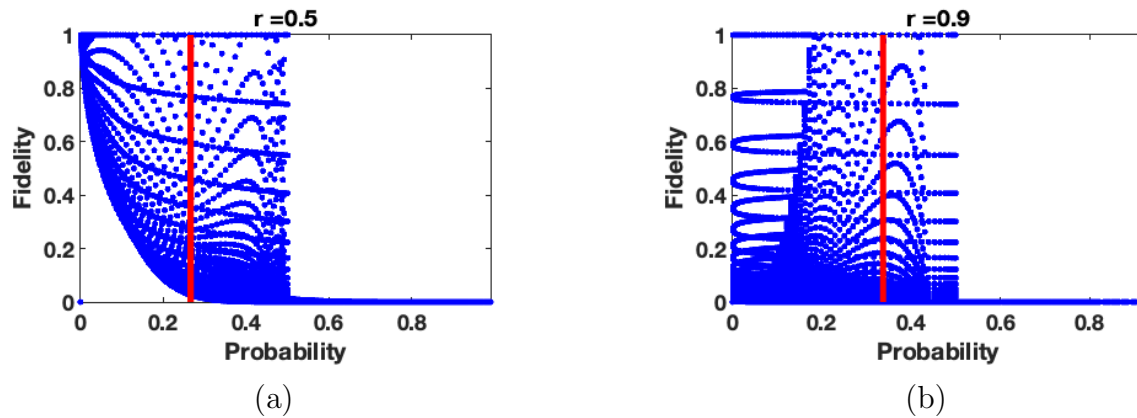


Figure 5. The relation between average total fidelity and average total probability. The solid red line represents the fidelity without any control. (a) $r = 0.5$. (b) $r = 0.9$.

As Fig. 5 depicted, the proposed scheme improves the amount of fidelity even for high decaying rates $r = 0.9$. However, for fidelity more than 0.5 the probability decreases to zero. Therefore, we can conclude that by setting optimum parameters, the maximum fidelity 0.5 is attainable with probability 1. One can gain fidelity more than 0.5 to 1 by giving up the probability (the probability is close to zero for fidelities more than 0.5).

4.2. Protection of generalized GHZ states

Above we mainly discuss the N -qubit GHZ state where $|\alpha| = |\beta|$, ($\gamma = \pi/2$) and $\phi_0 = 0$ in Eq. (5). If $|\alpha| \neq |\beta|$, ($\gamma \neq \pi/2$), it is non-maximally entangled state or generalized GHZ state. To find the behavior of proposed protection control for different initial generalized GHZ states, Fig. 6 shows the average total QFI for different amount of γ .

As Fig. 6 demonstrated, when $\alpha < \beta$ ($\pi/2 \leq \gamma < \pi$), the QFFCR can protect the QFI of phase for generalized GHZ states effectively for $r \leq 0.8$. When γ is close to $\pi/2$, the complete protection of QFI lasts for higher decaying rates, until $r = 0.9$. Also, the smaller the angle γ is, the lower QFI achieved.

As we show in subsection 3.1.2, by maximizing fidelity, the amount of probability decreases to zero. Hence, we study the behavior of fidelity for 10 qubits generalized GHZ state in case of maximizing probability. By setting the rotation angle as Eq. (17), we gain the probability 1, and maximum fidelity by finding optimum measurement

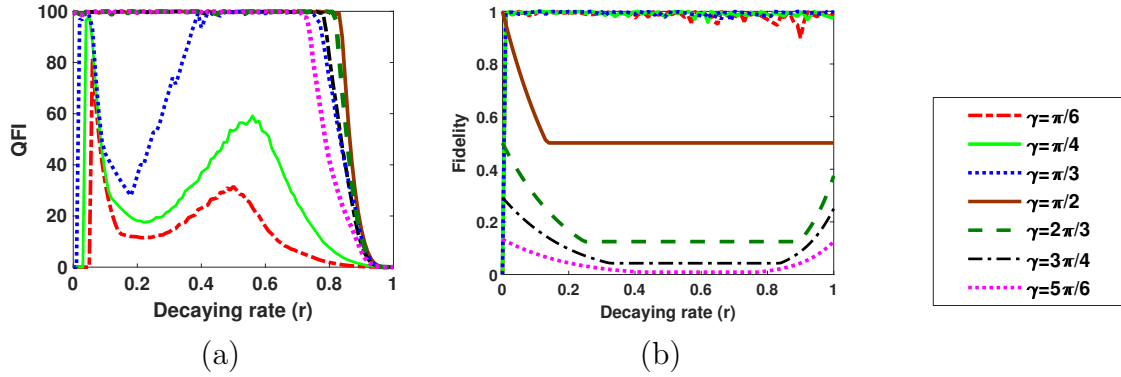


Figure 6. Average total QFI of phase and fidelity for different generalize GHZ states against amplitude damping for $N=10$.

angle θ for each decaying rate r . The Maximized fidelity according to probability 1 for different generalized GHZ states is given in Fig. 6(b). As Fig. 6(b) depicted, when $\alpha > \beta$ ($0 < \gamma \leq \pi/2$), the QFFCR can protect the generalized GHZ states completely and gain the average fidelity more than 99% and probability 1, even for intense decaying rates. Here again we note that, the corresponding probability of the plotted fidelities in Fig. 6(b) is 1.

Therefore, we can conclude that in case of generalized GHZ states protection, one cannot protect both the state and fidelity at the same time. However, by protecting each, the QFFCR give the best results for special states. The states that $\alpha > \beta$ ($0 < \gamma \leq \pi/2$) can be protected completely with almost complete fidelity and probability 1, even for high decaying rates; and the QFI of the states $\alpha < \beta$ ($\pi/2 \leq \gamma < \pi$), is protected significantly for $r \leq 0.8$.

5. Conclusion

In this paper, we study the protection of N -qubit GHZ and generalized GHZ states in ADC by means of weak measurement and offsetting operations. Before the state enters the ADC, we apply a weak measurement to obtain information about the state, and offsetting operation according to the result of the weak measurement to make the state less vulnerable to the effects of ADC. After the ADC, the same offsetting operation and a rotation operation are applied to retrieve the state. The final expressions to calculate the average total probability, fidelity and QFI for both GHZ state and generalized GHZ states are given. According to formulas we have shown that the proposed scheme can effectively protect the average QFI and the state of the N -qubit GHZ state and some generalized GHZ states. In case of protecting GHZ states, there is a trade-off between probability and fidelity, and with probability 1 the maximum fidelity 0.5 is attainable. For generalized GHZ states, when $\alpha < \beta$ ($\pi/2 \leq \gamma < \pi$), the proposed scheme can protect the QFI of phase effectively for $r \leq 0.8$; and when $\alpha > \beta$ ($0 < \gamma \leq \pi/2$) the states can be protected completely with almost complete fidelity and probability 1, even

for high decaying rates. Comparing our scheme with WMPPF shows the significant improvement of QFI protection in a probabilistic manner. Although WMPPF has the probability 1, our scheme notably increase the amount of QFI with acceptable probability even for intense decaying rates. Furthermore, our scheme is entirely feasible with current technology. The experimental realization of the weak measurement and correction rotation used in our scheme is discussed in [16].

Appendix

Density matrix of N -qubit GHZ state at each step of QFFCR

Here we derive the density matrix of the system at each step of the control procedure.

Here we assume that i qubits are measured by M_0^i and j qubits are measured by M_1^j , where $M_0^i = M_0$ and $M_1^j = M_1$ are given in Eq. (1). Hence, we define $i \in A$, $j \in B$, $A \cap B = \emptyset$, $A \cup B = \{1, \dots, N\}$, where A and B indicate a concrete combination of the qubits measured by M_0^i and M_1^j . A has k elements with $k = \{0, 1, \dots, N\}$ and B has $N - k$ elements. One case of measurement operator can be $M_{S_k} = \left[(M_0^i)^{\otimes k} \otimes (M_1^j)^{\otimes N-k} \right]_{S_k}$. If we fix the amount of k , M_{S_k} has $C_N^k = \frac{N!}{k!(N-k)!}$ combinations by changing the qubits, while the fixed number of qubits measured by M_0^i is k and the fixed number of qubits measured by M_1^j is $N - k$. The total combinations with all possible k is $C_N^0 + C_N^1 + \dots + C_N^N = 2^N$. The weak measurement set is a complete measurement, which $I^{\otimes 2N} = \sum_{k=0}^N \sum_{S_k=1}^{C_N^k} M_{S_k}^\dagger M_{S_k}$. By applying the weak measurement set for N qubits, there are 2^N cases which corresponds to a combination of $(M_0^i)^{\otimes k} \otimes (M_1^j)^{\otimes N-k}$, where k qubits are measured by M_0 and $N - k$ qubits measured by M_1 for $k = 0, 1, \dots, N$. Hence the weak measurement operator can be written as

$$\begin{aligned} M_{S_k} &= \left[(\cos(\theta/2)|0\rangle\langle 0| + \sin(\theta/2)|1\rangle\langle 1|)^{\otimes k} \otimes (\sin(\theta/2)|0\rangle\langle 0| + \cos(\theta/2)|1\rangle\langle 1|)^{\otimes N-k} \right]_{S_k} \\ &= \left[\begin{pmatrix} \cos(\theta/2) & 0 \\ 0 & \sin(\theta/2) \end{pmatrix}^{\otimes k} \otimes \begin{pmatrix} \sin(\theta/2) & 0 \\ 0 & \cos(\theta/2) \end{pmatrix}^{\otimes N-k} \right]_{S_k} \end{aligned} \quad (18)$$

In step 2 of the control procedure, the offsetting operations $F_0^i = F_0$ and $F_1^j = F_1$ are applied to qubits according to the result of the weak measurements M_0^i and M_1^j , respectively. Hence, the weak measurement and offsetting coupled operation is

$$\begin{aligned} U_{M-F} &= \left[(F_0^i)^{\otimes k} \otimes (F_1^j)^{\otimes N-k} (M_0^i)^{\otimes k} \otimes (M_1^j)^{\otimes N-k} \right]_{S_k} \\ &= \left[\begin{pmatrix} \cos(\theta/2) & 0 \\ 0 & \sin(\theta/2) \end{pmatrix}^{\otimes k} \otimes \begin{pmatrix} 0 & \cos(\theta/2) \\ \sin(\theta/2) & 0 \end{pmatrix}^{\otimes N-k} \right]_{S_k} \end{aligned} \quad (19)$$

The density matrix of the system after weak measurement and offsetting operations will

become

$$\begin{pmatrix} \ddots & & & & & \ddots \\ & W & & X & & \\ & & \ddots & \ddots & & \\ & & \ddots & \ddots & & \\ & Y & & Z & & \\ \ddots & & & & & \ddots \end{pmatrix} \quad (20)$$

where only four elements W, X, Y, Z are non-zero and all the other elements of the density matrix are zero. The amounts of four non-zero elements of the density matrix are

$$\begin{aligned} W &= |\alpha|^2 \left[\left(\begin{pmatrix} \cos^2(\theta/2) & 0 \\ 0 & 0 \end{pmatrix}^{\otimes k} \otimes \begin{pmatrix} 0 & 0 \\ 0 & \sin^2(\theta/2) \end{pmatrix}^{\otimes N-k} \right) \right]_{S_k}, \\ Z &= |\beta|^2 \left[\left(\begin{pmatrix} 0 & 0 \\ 0 & \sin^2(\theta/2) \end{pmatrix}^{\otimes k} \otimes \begin{pmatrix} \cos^2(\theta/2) & 0 \\ 0 & 0 \end{pmatrix}^{\otimes N-k} \right) \right]_{S_k}, \\ X &= \alpha\beta^* \left[\left(\begin{pmatrix} 0 & 0 \\ \cos(\theta/2)\sin(\theta/2) & 0 \end{pmatrix}^{\otimes k} \otimes \begin{pmatrix} 0 & \cos(\theta/2)\sin(\theta/2) \\ 0 & 0 \end{pmatrix}^{\otimes N-k} \right) \right]_{S_k}, \\ Y &= \alpha^*\beta \left[\left(\begin{pmatrix} 0 & \cos(\theta/2)\sin(\theta/2) \\ 0 & 0 \end{pmatrix}^{\otimes k} \otimes \begin{pmatrix} 0 & 0 \\ \cos(\theta/2)\sin(\theta/2) & 0 \end{pmatrix}^{\otimes N-k} \right) \right]_{S_k} \end{aligned} \quad (21)$$

Now the state goes through ADC. In this paper we assume that N qubits go through N independent amplitude damping channels which have the same damping probability $r_1 = r_2 = \dots = r_N = r$. For a general single-qubit ρ , amplitude damping can also be written as

$$\rho \rightarrow \varepsilon_{AD}(\rho) = e_0 \rho e_0^\dagger + e_1 \rho e_1^\dagger \quad (22)$$

According to Eq. (3) and (22), we conclude following effects of ADC

$$\begin{aligned} |0\rangle\langle 0| &= \begin{pmatrix} 1 & 0 \\ 0 & 0 \end{pmatrix} \rightarrow \begin{pmatrix} 1 & 0 \\ 0 & 0 \end{pmatrix}, \quad |1\rangle\langle 1| = \begin{pmatrix} 1 & 0 \\ 0 & 0 \end{pmatrix} \rightarrow \begin{pmatrix} r & 0 \\ 0 & 1-r \end{pmatrix} \\ |1\rangle\langle 0| &= \begin{pmatrix} 0 & 0 \\ 1 & 0 \end{pmatrix} \rightarrow \begin{pmatrix} 0 & 0 \\ \sqrt{1-r} & 0 \end{pmatrix}, \quad |0\rangle\langle 1| = \begin{pmatrix} 0 & 1 \\ 0 & 0 \end{pmatrix} \rightarrow \begin{pmatrix} 0 & \sqrt{1-r} \\ 0 & 0 \end{pmatrix} \end{aligned} \quad (23)$$

Hence, the elements of density matrix in Eq. (20) after passing through ADC

become

$$\begin{aligned}
W_e &= |\alpha|^2 \left[\begin{pmatrix} \cos^2(\theta/2) & 0 \\ 0 & 0 \end{pmatrix}^{\otimes k} \otimes \begin{pmatrix} \sin^2(\theta/2).r & 0 \\ 0 & \sin^2(\theta/2).(1-r) \end{pmatrix}^{\otimes N-k} \right]_{S_k}, \\
X_{e=\alpha\beta^*} &= \left[\begin{pmatrix} 0 & 0 \\ \cos(\theta/2) \sin(\theta/2)\sqrt{1-r} & 0 \end{pmatrix}^{\otimes k} \otimes \begin{pmatrix} 0 & \cos(\theta/2) \sin(\theta/2)\sqrt{1-r} \\ 0 & 0 \end{pmatrix}^{\otimes N-k} \right]_{S_k}, \\
Y_{e=\alpha^*\beta} &= \left[\begin{pmatrix} 0 & \cos(\theta/2) \sin(\theta/2)\sqrt{1-r} \\ 0 & 0 \end{pmatrix}^{\otimes k} \otimes \begin{pmatrix} 0 & 0 \\ \cos(\theta/2) \sin(\theta/2)\sqrt{1-r} & 0 \end{pmatrix}^{\otimes N-k} \right]_{S_k}, \\
Z_e &= |\beta|^2 \left[\begin{pmatrix} \sin^2(\theta/2).r & 0 \\ 0 & \sin^2(\theta/2).(1-r) \end{pmatrix}^{\otimes k} \otimes \begin{pmatrix} \cos^2(\theta/2) & 0 \\ 0 & 0 \end{pmatrix}^{\otimes N-k} \right]_{S_k}
\end{aligned} \tag{24}$$

After the ADC, the same offsetting operators are applied. So the state of the system after offsetting operations in step 4 of the control procedure are

$$\begin{aligned}
W_{e-f} &= |\alpha|^2 \left[\begin{pmatrix} \cos^2(\theta/2) & 0 \\ 0 & 0 \end{pmatrix}^{\otimes k} \otimes \begin{pmatrix} \sin^2(\theta/2).(1-r) & 0 \\ 0 & \sin^2(\theta/2).r \end{pmatrix}^{\otimes N-k} \right]_{S_k}, \\
X_{e-f=\alpha\beta^*} &= \left[\begin{pmatrix} 0 & \cos(\theta/2) \sin(\theta/2)\sqrt{1-r} \\ 0 & 0 \end{pmatrix}^{\otimes k} \otimes \begin{pmatrix} 0 & 0 \\ \cos(\theta/2) \sin(\theta/2)\sqrt{1-r} & 0 \end{pmatrix}^{\otimes N-k} \right]_{S_k}, \\
Y_{e-f=\alpha^*\beta} &= \left[\begin{pmatrix} 0 & 0 \\ \cos(\theta/2) \sin(\theta/2)\sqrt{1-r} & 0 \end{pmatrix}^{\otimes k} \otimes \begin{pmatrix} 0 & 0 \\ \cos(\theta/2) \sin(\theta/2)\sqrt{1-r} & 0 \end{pmatrix}^{\otimes N-k} \right]_{S_k}, \\
Z_{e-f} &= |\beta|^2 \left[\begin{pmatrix} \sin^2(\theta/2).r & 0 \\ 0 & \sin^2(\theta/2).(1-r) \end{pmatrix}^{\otimes k} \otimes \begin{pmatrix} 0 & 0 \\ 0 & \cos^2(\theta/2) \end{pmatrix}^{\otimes N-k} \right]_{S_k}
\end{aligned} \tag{25}$$

At the final step, we apply the correction rotation to retrieve the state. After the whole process of state protection, we can normalize the final state as:

$$\rho_f = \frac{1}{P} \tilde{\rho} = \frac{1}{P} \begin{pmatrix} A & 0 & D \\ 0 & E & 0 \\ C & 0 & B \end{pmatrix} \tag{26}$$

where $\tilde{\rho}$ is the unnormalized final state and P is the probability of appearing ρ_f . In ρ_f the four elements A, B, C, D are four corners of the density matrix with bases $|0\rangle \langle 0|^{\otimes N}, |1\rangle \langle 1|^{\otimes N}, |1\rangle \langle 0|^{\otimes N}, |0\rangle \langle 1|^{\otimes N}$ respectively. E is a diagonal matrix with $2^N - 2$ elements.

Here again we assume that k qubits are measured by M_0 and $N - k$ qubits are measured by M_1 . We give the elements of the final state in three cases:

- (i) When $k = 0$, all the qubits are measured by M_1 , the elements of the final state are

$$\begin{aligned} A_0 &= \left[|\alpha|^2 \sin^{2N} \left(\frac{\theta}{2} \right) e^{-N i \eta} (1-r)^N \right] |0\rangle\langle 0|^{\otimes N} \\ B_0 &= \left[e^{N i \eta} (|\alpha|^2 r^N \sin^{2N} \left(\frac{\theta}{2} \right) + |\beta|^2 \cos^{2N} \left(\frac{\theta}{2} \right)) \right] |1\rangle\langle 1|^{\otimes N} \\ C_0 &= D_0^\dagger = \alpha^* \beta (1-r)^{N/2} \frac{\sin^N(\theta)}{2^N} \\ E_0 &= \alpha^2 \sin^{2N} \left(\frac{\theta}{2} \right) * \\ &\quad \left[(e^{-i\eta}(1-r)|0\rangle\langle 0| + e^{i\eta}r|1\rangle\langle 1|)^{\otimes N} - e^{-N i \eta} (1-r)^N |0\rangle\langle 0|^{\otimes N} - e^{N i \eta} r |1\rangle\langle 1|^{\otimes N} \right] \end{aligned} \quad (27)$$

The probability of given final state is

$$P_0 = \alpha^2 \sin^{2N} \left(\frac{\theta}{2} \right) (r e^{N i \eta} + (1-r) e^{-N i \eta})^N + \beta^2 \cos^{2N} \left(\frac{\theta}{2} \right) e^{N i \eta} \quad (28)$$

- (i) If we assume $k = N$, which means all the qubits are measured by M_0 . In this case the elements of the final state are:

$$\begin{aligned} A_N &= \left[e^{N i \eta} (\alpha^2 \cos^{2N} \left(\frac{\theta}{2} \right) + \beta^2 r^N \sin^{2N} \left(\frac{\theta}{2} \right)) \right] |0\rangle\langle 0|^{\otimes N} \\ B_N &= \left[\beta^2 \sin^{2N} \left(\frac{\theta}{2} \right) e^{-N i \eta} (1-r)^N \right] |1\rangle\langle 1|^{\otimes N} \\ C_N &= D_N^\dagger = \alpha^* \beta (1-r)^{N/2} \frac{\sin^{2N}(\theta)}{2^N} \\ E_N &= \beta^2 \sin^{2N} \left(\frac{\theta}{2} \right) * \\ &\quad \left[(e^{i\eta}r|0\rangle\langle 0| + e^{-i\eta}(1-r)|1\rangle\langle 1|)^{\otimes N} - e^{N i \eta} r |0\rangle\langle 0|^{\otimes N} - e^{-N i \eta} (1-r)^N |1\rangle\langle 1|^{\otimes N} \right] \end{aligned} \quad (29)$$

With probability

$$P_N = \alpha^2 \cos^{2N} \left(\frac{\theta}{2} \right) e^{N i \eta} + \beta^2 \sin^{2N} \left(\frac{\theta}{2} \right) (r e^{i\eta} + (1-r) e^{-i\eta})^N \quad (30)$$

- (i) If we assume k qubits are measured by M_0 and $N - k$ qubits are measured by M_1 for $k = 1$ to $N - 1$, the elements of the final state are:

$$\begin{aligned} A_{S_k} &= \left[|\alpha|^2 \cos^{2k} \left(\frac{\theta}{2} \right) \sin^{2(N-k)} \left(\frac{\theta}{2} \right) (1-r)^{N-k} e^{(2k-N)i\eta} \right] |0\rangle\langle 0|^{\otimes N} \\ B_{S_k} &= \left[|\beta|^2 \sin^{2k} \left(\frac{\theta}{2} \right) \cos^{2(N-k)} \left(\frac{\theta}{2} \right) e^{(N-2k)i\eta} (1-r)^k \right] |1\rangle\langle 1|^{\otimes N} \\ C_{S_k} &= D_{S_k}^\dagger = \alpha^* \beta (1-r)^{N/2} \frac{\sin^N(\theta)}{2^N} \\ E_{S_k} &= |\alpha|^2 \sin^{2(N-k)} \left(\frac{\theta}{2} \right) \cos^{2k} \left(\frac{\theta}{2} \right) * \\ &\quad \left[e^{i k \eta} |0\rangle\langle 0|^{\otimes k} \otimes (e^{-i\eta}(1-r)|0\rangle\langle 0| + e^{i\eta}r|1\rangle\langle 1|)^{\otimes N-k} \right] + \\ &\quad |\beta|^2 \sin^{2k} \left(\frac{\theta}{2} \right) \cos^{2(N-k)} \left(\frac{\theta}{2} \right) * \\ &\quad \left[(e^{i\eta}r|0\rangle\langle 0| + e^{-i\eta}(1-r)|1\rangle\langle 1|)^{\otimes k} \otimes (e^{i\eta(N-k)}|1\rangle\langle 1|^{\otimes N-k}) \right] - A_{S_k} - B_{S_k} \end{aligned} \quad (31)$$

With probability:

$$\begin{aligned} P_{S_k} &= \alpha^2 \sin^{2(N-k)} \left(\frac{\theta}{2} \right) \cos^{2k} \left(\frac{\theta}{2} \right) e^{k i \eta} (r e^{i\eta} + (1-r) e^{-i\eta})^{N-k} \\ &\quad + \beta^2 \cos^{2(N-k)} \left(\frac{\theta}{2} \right) e^{(N-k)i\eta} \sin^{2k} \left(\frac{\theta}{2} \right) (r e^{i\eta} + (1-r) e^{-i\eta})^{N-k} \end{aligned} \quad (32)$$

Acknowledgments

This work was partially supported by the National Natural Science Foundation of China under Grant 61973290 and Grant 61720106009. The research of J. J. Nieto has been partially supported by the Agencia Estatal de Investigacion (AEI) of Spain, project PID2020-113275GB-I00, co-financed by the European Fund for Regional Development (FEDER); and by Xunta de Galicia under grant ED431C 2019/02.

Acknowledgments

References

- [1] Tóth G and Apellaniz I 2014 Quantum metrology from a quantum information science perspective *J. Phys. A Math. Theor.* **47** 424006
- [2] Harraz S, Cong S and Li K 2020 Online quantum state tomography of N -qubit via continuous weak measurement and compressed sensing *Int. J. Quantum Inf.* **2040006** 1–18
- [3] Harraz S and Cong S 2019 State transfer via on-line state estimation and Lyapunov-based feedback control for a N -qubit system *Entropy* **21**
- [4] Seveso L, Albarelli F, Genoni M G and Paris M G A 2019 On the discontinuity of the quantum Fisher information for quantum statistical models with parameter dependent rank *J. Phys. A Math. Theor.* **53** 02LT01
- [5] Braunstein S L and Caves C M 1994 Statistical distance and the geometry of quantum states *Phys. Rev. Lett.* **72** 3439–43
- [6] Hao X, Tong N-H and Zhu S 2013 Dynamics of the quantum Fisher information in a spin-boson model *J. Phys. A Math. Theor.* **46** 355302
- [7] Liu J, Yuan H, Lu X-M and Wang X 2019 Quantum Fisher information matrix and multiparameter estimation *J. Phys. A Math. Theor.* **53** 23001
- [8] Altafini C and Ticozzi F 2012 Modeling and control of quantum systems: An introduction *IEEE Trans. Automat. Contr.* **57** 1898–917
- [9] Cong S 2014 *Control of Quantum Systems: Theory and Methods* (John Wiley & Sons)
- [10] Liao Z, Al-Amri M and Zubairy M S 2013 Protecting quantum entanglement from amplitude damping *J. Phys. B At. Mol. Opt. Phys.* **46** 145501
- [11] Wagner T, Kampermann H and Bruß D 2018 Analysis of quantum error correction with symmetric hypergraph states *J. Phys. A Math. Theor.* **51** 125302
- [12] Hammond A M, Frank I W and Camacho R M 2018 Error correction in structured optical receivers *IEEE J. Sel. Top. Quantum Electron.* **24** 1–8
- [13] Grassl M, Kong L, Wei Z, Yin Z-Q and Zeng B 2018 Quantum error-correcting codes for qudit amplitude damping *IEEE Trans. Inf. Theory* **64** 4674–85
- [14] Forney G D, Grassl M and Guha S 2007 Convolutional and Tail-Biting Quantum Error-Correcting Codes *IEEE Trans. Inf. Theory* **53** 865–80
- [15] Ofek N, Petrenko A, Heeres R, Reinhold P, Leghtas Z, Vlastakis B, Liu Y, Frunzio L, Girvin S M and Jiang L 2016 Extending the lifetime of a quantum bit with error correction in superconducting circuits *Nature* **536** 441
- [16] Cramer J, Kalb N, Rol M A, Hensen B, Blok M S, Markham M, Twitchen D J, Hanson R and Taminiau T H 2016 Repeated quantum error correction on a continuously encoded qubit by real-time feedback *Nat. Commun.* **7**
- [17] Chao R and Reichardt B W 2018 Quantum error correction with only two extra qubits *Phys. Rev. Lett.* **121** 50502
- [18] Cong S and Yang F 2013 Control of quantum states in decoherence-free subspaces *J. Phys. A Math. Theor.* **46** 75305

- [19] Chen C, Yang C-J and An J-H 2016 Exact decoherence-free state of two distant quantum systems in a non-Markovian environment *Phys. Rev. A* **93** 62122
- [20] Chen M, Kuang S and Cong S 2017 Rapid Lyapunov control for decoherence-free subspaces of Markovian open quantum systems *J. Franklin Inst.* **354** 439–55
- [21] Zhang J, Wu R-B, Li C-W and Tarn T-J 2010 Protecting coherence and entanglement by quantum feedback controls *IEEE Trans. Automat. Contr.* **55** 619–33
- [22] Brańczyk A M, Mendonça P E M F, Gilchrist A, Doherty A C and Bartlett S D 2007 Quantum control of a single qubit *Phys. Rev. A* **75** 1–11
- [23] Gillett G G, Dalton R B, Lanyon B P, Almeida M P, Barbieri M, Pryde G J, O’Brien J L, Resch K J, Bartlett S D and White A G 2010 Experimental feedback control of quantum systems using weak measurements *Phys. Rev. Lett.* **104** 3–6
- [24] Vuglar S L and Petersen I R 2016 Quantum noises, physical realizability and coherent quantum feedback control *IEEE Trans. Automat. Contr.* **62** 998–1003
- [25] Wen J, Shi Y, Pang X, Jia J and Zeng J 2020 Rapid stabilization of time delay stochastic quantum systems based on continuous measurement feedback *J. Franklin Inst.* **357** 7515–36
- [26] Qamar S and Cong S 2019 Observer-based feedback control of two-level open stochastic quantum system *J. Franklin Inst.* **356** 5675–91
- [27] Wang C, Xu B, Zou J, He Z, Yan Y, Li J and Shao B 2014 Feed-forward control for quantum state protection against decoherence *Phys. Rev. A* **89** 032303
- [28] Cao Y, Tian G, Zhang Z, Yang Y, Wen Q and Gao F 2017 Composite control for protecting two nonorthogonal qubit states against decoherence *Phys. Rev. A* **032313** 1–9
- [29] Guo L S, Xu B M, Zou J, Wang C Q, Li H, Li J G and Shao B 2015 Discriminating two nonorthogonal states against a noise channel by feed-forward control *Phys. Rev. A - At. Mol. Opt. Phys.* **91** 1–11
- [30] Harraz S, Cong S and Shuang F 2018 Quantum noise protection via weak measurement for quantum mixed states *Proceedings of 2018 IEEE 7th Data Driven Control and Learning Systems Conference, DDCLS 2018* pp 302–7
- [31] Harraz S, Cong S and Kuang S 2019 Optimal Noise Suppression of Phase Damping Quantum Systems via Weak Measurement *J. Syst. Sci. Complex.* **32** 1264–79
- [32] Harraz S, Cong S and Li K 2020 Two-qubit state recovery from amplitude damping based on weak measurement *Quantum Inf. Process.* **19** 1–22
- [33] Harraz S, Yang J, Li K and Cong S 2017 Quantum state transfer control based on the optimal measurement *Optim. Control Appl. Methods* **38** 744–53
- [34] Qi B, Pan H and Guo L 2012 Further results on stabilizing control of quantum systems *IEEE Trans. Automat. Contr.* **58** 1349–54
- [35] Ritchie N W M, Story J G and Hulet R G 1991 Realization of a measurement of a “weak value” *Phys. Rev. Lett.* **66** 1107
- [36] Harraz S and Cong S 2020 N-Qubit State Protection against Amplitude Damping by Quantum Feed-Forward Control and its Reversal *IEEE J. Sel. Top. Quantum Electron.* **26**
- [37] Chen Y, Zou J, Long Z W and Shao B 2017 Protecting quantum Fisher information of N -qubit GHZ state by weak measurement with flips against dissipation *Sci. Rep.* **7** 1–12
- [38] d’Alessandro D 2007 *Introduction to quantum control and dynamics* (CRC press)
- [39] Genoni M G, Olivares S and Paris M G A 2011 Optical phase estimation in the presence of phase diffusion *Phys. Rev. Lett.* **106** 1–4